A Study of Icariin Modulating Hippocampal Neurogenesis in Depression Based on Quantitative CSF Proteomics

Ning-Xi Zeng
Guangzhou University of Chinese Medicine
Huizhen Li
Guangzhou University of Chinese Medicine
Han-Zhang Wang
Guangzhou University of Chinese Medicine
Kai-Ge Liu
Guangzhou University of Chinese Medicine
Xia-Yu Gong
Guangzhou University of Chinese Medicine
Wu-Long Luo
Guangzhou University of Chinese Medicine
Can Yan
Guangzhou University of Chinese Medicine
Li-Li Wu (wulili@gzucm.edu.cn)
Guangzhou University of Chinese Medicine https://orcid.org/0000-0002-8097-1960

Research

Keywords: depression, hippocampal neurogenesis dysfunction, cerebrospinal fluid, proteomics, Icariin

Posted Date: October 1st, 2020

DOI: https://doi.org/10.21203/rs.3.rs-80131/v1

Abstract

Background

Hippocampal neurogenesis dysfunction is one of the main pathogenesis of depression. Icariin (ICA) has significant anti-depression and anti-hippocampal damage effects but could not effectively cross the blood-brain-barrier and accumulate in brain. Based on the proteomics of cerebrospinal fluid (CSF), this study aimed to explore the mechanism of ICA against hippocampal neurogenesis dysfunction in depression.

Methods

In vivo, rats were exposed to 6-week CUMS and treated by ICA to observe the effects of ICA on depressive symptoms, cognitive functions, neurogenesis and number of neurons in DG. Tandem mass tag (TMT) proteomics were used to screen the differentially expressed proteins (DEPs) in CSF co-regulated by CUMS and ICA. Parallel reaction monitoring (PRM) was used to validate 10 DEPs that were related to cell proliferation and survival. In vitro, CSF was conducted on primary hippocampal neural stem cells (NSCs) to observe the proliferation and differentiation under high-corticosterone (CORT) concentration.

Results

It was shown that ICA could alleviate depressive symptoms, learning-memory dysfunction, neurogenesis dysfunction and neuronal loss in DG of depression rats and ICA-CSF could effectively repair the CORT-induced damage. A total of 52 DEPs co-regulated by CUMS and ICA in CSF were screened and mainly involved in ribosome pathway, PI3K-Akt pathway and IL-17 pathway. Rps4x, Rps12, Rps14, Rps19, Hsp90b1, Hsp90aa1 and HtrA1 were validated by PRM.

Conclusions

These findings indicate that to regulate the expression of proteins in CSF may be involved in the effects of ICA against hippocampal neurogenesis dysfunction in depression.

1. Introduction

Depression is one of the most common mental disorders, mainly characterized by despair, anhedonia and even suicide attempts[1]. With the increase of life pressure and social stress, the prevalence and morbidity of depression continue to rise. It has generated huge burdens on individuals, families and society, causing worldwide attention. Depression is a psychologic disease with complex etiology and clinical manifestations, so far, its pathogenesis has not been fully elucidated.

Hippocampal damage is currently recognized as one of the pathogenesis of depression, and hippocampal neurogenesis dysfunction plays an important role in it [2-4]. It has been found by clinical autopsy that the hippocampus volume reduced with severe neuronal loss or atrophy in depression patients[5]. Preclinical researches proved that the branches number and the length of hippocampal neurons dendritic were reduced and neurogenesis was impaired in depression animals[6, 7]. Therefore, how to repair hippocampal damage has become the focus of current anti-depression treatment[8].

Icariin (ICA) is one of the most dominating bioactive constituents in *Herba epimedii*. Recently, plenty of evidence confirmed that ICA could effectively alleviate depressive symptoms and protect hippocampus by relieving neuroinflammation and repairing hypothalamic–pituitary–adrenal axis dysfunction [9-11]. However, studies have shown that ICA could not effectively cross the blood-brain barrier and always eliminated rapidly and thus it accumulated very little in brain[12]. Except the mild direct effect on the brain parenchyma, whether ICA protects hippocampus in depression by other approach.

Cerebrospinal fluid (CSF) is the ultrafiltrate from plasma, which is in direct contact with the central nervous system (CNS). CSF is bound up with hippocampus which is adjacent to the lateral ventricle. The substances in CSF may directly affect structure and function of hippocampus, such as regulating neurogenesis[13, 14]. CSF plays an important role in molecular exchange and signal transmission in the CNS. Consequently, the alteration of CSF components might result in the occurrence and development of CNS diseases [15-17]. As is known that the proteomics of CSF changed in patients with depression and the differential expressed proteins were closely linked to the damage and dysfunction of the CNS [18, 19].

Based on the relationship among the alteration of CSF components, depression and hippocampal damage, it was hypothesized that ICA might influence brain parenchyma through the limbic regions of brain, such as CSF and choroid plexus, and exert anti-depression and against hippocampal damage.

To verify this hypothesis, *in vivo*, chronic unpredictable mild stress (CUMS) model was applied to observe the effects of ICA on anti-depression and hippocampal protection. The proteomics were used to screen the differentially expressed proteins (DEPs) in CSF co-regulated by CUMS and ICA. *In vitro,* the stress damage of neural stem cells (NSCs) was simulated under the high-CORT concentration, and the effect of ICA-treated CSF on proliferation and differentiation of NSCs under high-CORT concentration was explored. Through the above experiments, this study aimed to explore the mechanism of ICA against hippocampal damage in depression.

2. Materials And Methods

2.1 Animals

A total of 45 male Wistar rats weighing 180–220 g and aged 7–8 weeks (License No. SCXK (Yue) 2016-0041) were obtained from the Laboratory Animal Center of Southern Medical University, Guangzhou, China. Rats were housed (5 per cage) for 1 week for acclimation to the environment (23 ±2℃; 48-60% humidity; and on a 12 h light/12 h dark cycle) with diet and water available. All experimental procedures and protocols were approved by the Experimental Animal Ethics Committee of Guangzhou University of Chinese Medicine of China. The experimental procedure followed the United States National Institutes of Health Guide for the Care and Use of Laboratory Animals (NIH Publication No. 85-23, revised 1996).

2.2 Drugs and treatment groups in vivo

After adaption for one week, all rats were solitary-housed for sucrose preference test (SPT; as described in *2.4 Sucrose preference test (SPT)*). Unqualified rats were excluded according to the following SPT results: low sucrose preference (less than 60%), location preference (preferred to drink liquid from a fixed location), drinking too little (drinking neither sucrose solution nor pure water) and excessive drinking (total liquid consumption more than twice the average total liquid consumption of all rats).

Rats were randomly divided into three groups based on body weight and sucrose preference: the control group (CON, n=15), the CUMS group (CUMS, n= 15) and the ICA group (ICA, n=15).

ICA (Dilger, Nanjing, China; purity≥98%) was dissolved into a suspension (30 mg/mL) with normal saline. Rats in the ICA group were intragastrically administrated with ICA at a dose of 120 mg/kg and the CON group and CUMS group were intragastrically treated with the same volume of normal saline at 16:00 every day during CUMS modeling.

2.3 CUMS procedures

Rats in the control group were housed 5 per cage and underwent normal feeding without any stressors. Rats in the CUMS and ICA group were solitary-housed and subjected to CUMS for 6 weeks. According our previous study[4], the CUMS procedures were adopted and modified. In brief, rats were randomly exposed to 1–2 of these stimuli once a day for 6 weeks and the same stressors were not scheduled in three consecutive days (**as shown in figure 1**). Stressors included white noise (85 dB, 5 hours); thermal swimming (45°C, 5 min); stroboscopic illumination (300 flashes/minute, 5 h); soiled cage (10 h); paired with four other stressed animals (10 h); cold swimming (4 ℃, 5 min); tail pinching (3 min); restraint (12 h); water deprivation (12 hours) and food deprivation (12 or 24 hours).

After the 6-week CUMS, behavior tests were carried out, CSF sample and hippocampus slides were prepared (**as shown in figure 2**).

2.4 Sucrose preference test (SPT)

The procedure was performed to assess rats' anhedonia according to our previous method[4]. During the SPT, all rats were kept in single cages. The sucrose preference test was divided into four stages: sucrose training for 48 hours, baseline testing for 36 hours, food and water deprivation for 24 hours, and sucrose preference testing for 12 hours. Two bottles of liquid (1% sucrose solution and pure water) were given to each animal at the same time during the test. In the sucrose preference test stage, after 12 hours of liquid availability (20:30–8:30 the next day), the consumed volume of each solution was recorded to calculate sucrose preference. Sucrose preference (%) = sucrose solution consumption/total liquid intake × 100%.

2.5 Open field test (OFT)

Open-field test was performed to assess locomotor activity referred to our previous method[4]. The rats were transferred to the behavioral test room (soundproof darkroom) before the OFT for habituation to the environment for 1 hour. Each rat was individually placed into the middle of the open-field apparatus (100 cm ×100 cm ×48 cm) and then allowed to explore freely for 5 minutes. The total traveling distance was recorded by video-tracking system (Flydy Co.,Ltd, Guangzhou, China).

2.6 Forced swimming test (FST)

The immobility time in FST was used to evaluate the desperation. The procedure was referred to our previous method [20]. The rats habituated an hour in the behavioral test room before the test. During FST, the rats were individually placed in a transparent plexiglas cylinder (height: 100 cm, diameter: 30 cm) filled with 35 cm water (25±1 ℃) and forced to swim for 6 min. The immobility time during the last 4 minutes was recorded by three

researchers blind to the experimental design. Rats were considered immobile when they ceased struggling and remained floating motionless in the water except the movements necessary to keep their heads above the water.

2.7 T-maze test [21]

T-maze test was used to evaluate learning and memory ability. The T-maze equipment was constructed of T-shaped elevated maze with a start arm (71cm ×18 cm×30 cm) and two target arms (46cm×18 cm×30cm) made of black and non-reflective panels. Light was avoided throughout the test. The rats were food-deprived and received approximately 75% of common daily intake food during the T-maze test. The T-maze test was divided into the training and testing phases. During the training phase, cheeses were placed at the end of both target arms with both doors open. The rats were placed in the start arm and allowed to freely explore the maze and intake cheese. During the testing phase, cheeses were placed at the end of both target arms. The door of one random target arm namely goal arm was closed. The rat was placed in the start arm and allowed to eat the cheese in the opened target arm. Once the rat entered the opened target arm, the door was closed immediately. The rat was taken out after eating the cheese. Thirty seconds later, the rat was placed in the start arm again and allowed to freely explore the maze with both doors open. If the rat entered the goal arm and finished eating the cheese, it was scored as 1 correct time. The testing phase was repeated 10 times a day (each interval was 20 minutes) and lasted for 4 days. Accuracy (%) = correct times/10 × 100%.

2.8 CSF sample preparation

CSF sample was prepared 24 hours after the T-maze test. The rats were anesthetized and exposed the foramen magnum. intravenous infusion needle (0.45#) was attached to syringe (1mL). CSF was collected from cisterna magna puncture, centrifuged at 3000 rpm for 15 min at 4 °C. The supernatant of CSF was collected and frozen at -80 °C.

2.9 Immunofluorescence of sections

Referred to our previous experimental approach[4], 5-Bromo-2-deoxyUridine (BrdU, Sigma, US) was intraperitoneally injected (three injections, 4 hours apart, 200 mg/kg). One week later, the brain tissues (2.7mm-6.7mm from coronal groove) were dissected and fixed in 4% paraformaldehyde for 24 hours at 4°C and then immersed in 30% sucrose until sank to the bottom. The hippocampus was trimmed according to the coronary sulcus (2.7mm-6.7mm from coronal sulcus), and was cut into 40 μm-thick frozen slices.

BrdU /doublecortin (DCX) double labeling was used to label the new-born precursor neurons, reflecting the abilities of proliferation and differentiation into neuron of NSCs in DG. Sections were treated with 2M HCL for 20 minutes at 37 °C, washed thrice in phosphate buffer saline (PBS 0.1 M, pH 8.4), blocked in 5% goat serum (containing 0.03% Triton-X-100) at room temperature for 1 hour and incubated with rat anti-BrdU antibody (1:200, Abcam, UK) and rabbit anti-DCX antibodies (1:200, Abcam, UK) at 4° C overnight. After washed in Tris-buffered saline with 0.01% Tween-20, the sections were incubated with AlexaFluor® 594 goat anti-rat antibodies (1:500, Abcam, UK) and AlexaFluor® 488 goat anti-rabbit (1:500, Abcam, UK) at 37°C for 2 hours. After washed and 4',6-diamidino-2-phenylindole (DAPI) staining, images were captured by laser confocal microscope (LSM800, ZEISS, Germany). The number of BrdU/DCX positive cells were record.

NeuN was used to label mature neurons and to reflect the number of neurons in DG. The sections were rewarmed, membrane-ruptured with Triton-X, blocked with goat serum and incubated with rabbit anti-NeuN antibody (1:1000, Abcam, UK) overnight at 4 ℃. After washed in TBST, the sections were incubated with AlexaFluor® 488 goat anti-rabbit (1:500, Abcam, UK) at 37°C for 2 hours. After washing and DAPI staining, images were captured by laser confocal microscope (LSM800, ZEISS, Germany). Ratio of NeuN positive cells (%)= NeuN positive cell number/total number of nuclei×100%.

2.10 Culture of primary hippocampal NSCs

The embryo was removed from Wistar rats (obtained from the Laboratory Animal Center of Southern Medical University, Guangzhou, China) at pregnant days 16–18 under sterile conditions by etherization and placed in ice-cold sterile PBS. The bilateral hippocampus was separated, cut into 1 mm × 1 mm × 1 mm pieces, mixed and gently polished with a Pasteur pipette, filtered through a 200-mesh cell sieve to obtain a single cell suspension, and centrifuged at 1200 rpm for 5 minutes. After the supernatant was discarded, the cells were resuspend with neural stem cell medium (DMEM/F12 supplemented with 20 ng/L EGF(Gibco, US), 20 ng/L bFGF(Gibco, US), 2% B27(Gibco, US) and 1% Penicillin /Streptomycin (Gibco, US)). Cells were incubated at a density of 2×10^5 cells/mL in 60 mm culture dishes at 37°C in a 5% (v/v) CO2 incubator. The culture medium was half-replenished every 2–3 days.

2.11 Cell Counting Kit-8 (CCK-8) test

P1-generation NSCs were collected and divided into 5 groups, control group (cultured with neural stem cell medium (DMEM/F12 containing 20 ng/L EGF, 20 ng/L bFGF, 2% B27 and 1% Penicillin /Streptomycin)), high-CORT concentration group (cultured with neural stem cell medium containing 100 μM CORT (Millipore, US)), CON-CSF- group (cultured with neural stem cell medium containing 20% CON-CSF +100 μM CORT), CUMS-CSF group (cultured with neural stem cell medium containing 20% CUMS-CSF +100 μM CORT), and ICA-CSF group(cultured with neural stem cell medium containing 20% ICA-CSF +100 μM CORT).

Cell viability was detected by CCK-8. Referred to our previous method (Wu et.al., 2013), passage1 neutrospheres were digested into single cells by Accutase^{TM} (Gibco, US), resuspended with neural stem cell medium and seeded in 96-well plates at a density of 4×10^4cells/well. Required CSF and CORT were added into each group, the final volume of culture medium was 100 μL per well. After 72 h, 10 μL of CCK-8 (Dojindo, Japan) was added to each well and cells were cultured for 2 h. NSCs were dispersed into single cells by enzyme, resuspended with neural stem cell culture medium and seeded into 96-well plates at a density of 4×10^4 cells per well. The optical density (OD) was measured at 450 nm with a microplate reader (Bio-rad, US). The cell viability was calculated as following: cell viability (%) = [OD (experiment)-OD (blank)] / [OD (control) – OD (blank)] ×100%.

2.12 Immunofluorescence of primary hippocampal NSCs

Previous studies usually selected media containing 10% fetal bovine serum (FBS) as differentiation medium[8]. Considering that CSF has a certain role in promoting the differentiation of NSCs, NeuralBasal (Gibco, US) containing 2% FBS (Gibco, US) was used as a differentiation culture medium in this study. P1-generation neural stem cells were collected and divided into 7 groups, control group 1 (cultured with NeuralBasal containing 10% FBS), control group 2 (cultured with NeuralBasal containing 2% FBS), control group 3 (cultured with NeuralBasal containing 2% FBS +20% normal CSF), high-CORT concentration group (cultured with NeuralBasal containing 2%

FBS +100 μM CORT), CSF of CON group (cultured with NeuralBasal containing 2% FBS +100 μM CORT +20% CSF of CON), CSF of CUMS group (cultured with NeuralBasal containing 2% FBS +100 μM CORT +20% CSF of CUMS), and CSF of ICA group (cultured with NeuralBasal containing 2% FBS +100 μM CORT +20% CSF of ICA).

Referring to our previous method[8], NSCs were dispersed into single cells by Accutase™ and resuspended with the differentiation culture medium (NeuralBasal containing 2% FBS) and then seeded into 15 mm confocal dishes (5000 cells/dish). After 48 h, the CORT and CSF were added as required for each group. The incubation was continued for another 48 h, 10 μM BrdU was added to each dish. After 48 h, 4% paraformaldehyde was fixed and BrdU/DCX was labeled by Immunofluorescence, as described in step 2.9.

2.13 Tandem mass tag (TMT) analysis of CSF proteomics

Protein was extracted from cerebrospinal fluid. After quantification and separation, 30 μL protein was taken from each sample for proteolysis. TMT labeling was carried out in accordance with the instructions of the TMT labeling kit (Thermo, US). High pH RP spin column was used for grading. The samples were separated by chromatography (Thermo, US) and analyzed by mass spectrometry (Thermo, US). The original data were identified and quantitatively analyzed by Mascot2.2 and Proteome Discoverer1.4. Proteins with a fold change more than 1.2 or less than 0.83 as well as a statistical P-value < 0.05 between two groups were selected as DEPs.

2.14 Bioinformatic analysis

Gene Ontology (GO) mapping and annotation of proteins were conducted using the Blast2GO. Kyoto Encyclopedia of Genes and Genomes (KEGG) annotation were was performed using KAAS (KEGG Automatic Annotation Server). Enrichment analysis was performed by Fisher's Exact Test with P-values less than 0.05 and an FDR value less than 0.5.

2.15 Parallel reaction monitoring (PRM) quantitative analysis of target protein

The proteins of CSF samples were extracted and hydrolyzed and then separated by HPLC system (Thermo, USA). The separated peptides were analyzed by PRM mass spectrometry (Thermo, USA). The PRM test was repeated three times. Finally, the software Skyline3.7.0 was used to analyze the data of the original PRM file and to quantify the target protein and target peptide.

2.16 Statistical analysis

The data were statistically analyzed using SPSS 22.0 software (IBM, USA). All results were expressed as the mean ± SEM. The data of each group were consistent with a normal distribution (Shapiro-Wilk test). An independent samples t-test was used for comparisons between two groups with homogeneity of variance；one-way ANOVA was used for comparisons between three or more groups with homogeneity of variance, and Welch's test was used for heterogeneity of variance. In the pairwise comparisons, the LSD test was used to assess results with homogeneity of variance, and the Games-Howell method was used to assess results with heterogeneity of variance. T-maze accuracy was analyzed by repeated-measures ANOVA. The Greenhouse-Geisser correction was used when the assumption of sphericity was not met. Comparisons of the accuracy between groups at each individual time point were conducted using a multivariate ANOVA. P-values<0.05 were considered statistically significant.

3. Results

3.1 ICA could reverse the depression-like behaviors of CUMS rats

3.1.1 The effect of ICA on sucrose preference of CUMS rats

As shown in Figure 3A, compared with the CON group, sucrose preference of the CUMS group was significantly decreased (n=15, $F_{(2, 42)}$=27.476, p<0.01); compared with the CUMS group, sucrose preference of the ICA group was significantly increased (n=15, $F_{(2, 42)}$=27.476, p<0.01), indicating that ICA could alleviate the anhedonia symptom of CUMS rats.

3.1.2 The effect of ICA on total distance in the OFT of CUMS rats

As shown in Figure 3B, compared with the CON group, CUMS significantly reduced the total traveled distance (n=15, $F_{(2, 42)}$= 34.641, p<0.01) in the OFT. Compared with the CUMS group, ICA significantly elevated the total traveled distance (n=15, $F_{(2, 42)}$= 34.641, p<0.01), suggesting that ICA had a significant effect on improving the locomotor activity of CUMS rats.

3.1.3 The effect of ICA on immobility time of the FST in CUMS rats

As shown in Figure 3C, the immobility time in rats with CUMS increased significantly (n=15, $F_{(2, 42)}$= 24.394, p<0.01) compared with the control group. ICA significantly decreased the immobility time (n=15, $F_{(2, 42)}$= 24.394, p<0.01) compared with the control group. It was suggested that ICA treatment could alleviate the desperation of CUMS rats.

3.2 ICA could alleviate hippocampal damage in CUMS rats

3.2.1 Effect of ICA on T-maze accuracy in CUMS rats

As shown in Figure 4A, compared with the CON group, there was no difference in the accuracy of the CUMS group in Day1 and a significant reduction of the accuracy in Day2-4. (n=7-10. Day2, $F_{(2, 21)}$=8.859, p<0.01; Day3, $F_{(2, 21)}$=4.612, p<0.01; Day4, $F_{(2, 21)}$=5.998, p<0.01). Compared with the CUMS group, the accuracy of the ICA group in Day 2-4 was significantly improved (n=7-10. Day2, $F_{(2, 21)}$=8.859, p=0.0447; Day3, $F_{(2, 21)}$=4.612, p<0.01; Day4, $F_{(2, 21)}$=5.998, p=0.0234). It was suggested that ICA treatment could repair the learning and memory impair of CUMS rats.3.2.2 Effect of ICA on neurogenesis dysfunction in DG in CUMS rats

3.2.2 Effect of ICA on number of BrdU/DCX positive cells in DG in CUMS rats

As shown in Figure 4B and 4C, compared with the CON group, the number of BrdU/DCX positive cells in DG of the CUMS group reduced significantly (n=5, $F_{(2, 12)}$=53.44, p<0.01). Compared with the CUMS group, ICA significantly increased the number of BrdU/DCX positive cells in DG (n=5, $F_{(2, 12)}$=53.44, p<0.01). It was indicated that ICA treatment could alleviate CUMS-induced neurogenesis dysfunction in DG.

3.2.3 Effect of ICA on relatively number of neurons in DG in CUMS rats

As shown in figure 4D and 4E, compared with the CON group, the relatively number of neurons in DG of the CUMS group reduced significantly (n=4-5, $F_{(2, 12)}$=27.68, p<0.01). Compared with the CUMS group, ICA significantly increased the relatively number of neurons (n=4-5, $F_{(2, 12)}$=27.68, p<0.01). It was suggested that ICA treatment could resist neuronal reduction in DG.

3.3 Effect of ICA CSF on the proliferation and differentiation of neural stem cells under high-CORT concentration

3.3.1 Effect of ICA CSF on the proliferation of NSCs under high-CORT concentration

As shown in Figure5A, compared with the control group, the vitality of NSCs in the CORT group was significantly reduced (n=10, $F_{(4, 45)}$=53.41, p<0.01). Compared with CORT group, the NSCs viability of the CON-CSF group (n=10, $F_{(4, 45)}$=53.41, p<0.01) and the ICA-CSF group (n=10, $F_{(4, 45)}$=53.41, p=0.021) was significantly increased. There was no significant change between CORT group and CUMS-CSF group, suggesting CON-CSF and ICA-CSF could promote the proliferation of NSCs under high-CORT concentration. But CUMS-CSF had no significant effect. Compared with the CUMS-CSF group, the cell viability of NSCs in the ICA-CSF group was significantly increased.

3.3.2 Effect of ICA CSF on the proliferation of NSCs into neurons under high-CORT concentration

As shown in Figure 5B, 5C and 5D, compared with the control group 1 (10% FBS), the number of BrdU positive cells (n=5-6, $F_{(6, 29)}$=48.32, p=0.22) and the proportion of BrdU/DCX double-positive cells (n=4-7, $F_{(6, 29)}$=15.34, p<0.01)in the control group 2 (2% FBS) were significantly reduced, while there was no significant difference in control group 3 (2% FBS + 20% normal CSF). Compared with the control group 2, the number of BrdU positive cells (n=4-7, $F_{(6, 29)}$=48.32, p=0.03) and the ratio of BrdU/DCX double-positive cells (n=4-7, $F_{(6, 29)}$=15.34, p=0.12) in the control group 3 increased significantly. It was suggested that normal CSF could promote the proliferation and differentiation of NSCs.

Compared with the CORT group, the number of BrdU positive cells (n=4-7, $F_{(6, 29)}$=48.32, p<0.01) and the ratio of BrdU/DCX double-positive cells (n=4-7, $F_{(6, 29)}$=15.34, p<0.01) in the CON-CSF group were significantly increased but CUMS-CSF group showed no significant change.

Compared with the CON-CSF group, the number of BrdU positive cells (n=4-7, $F_{(6, 29)}$=48.32, p<0.01) and the ratio of BrdU/DCX double-positive cells (n=4-7, $F_{(6, 29)}$=15.34, p<0.01) in the CUMS-CSF group were significantly reduced while there was no significant change in the ICA-CSF group. Compared with the CUMS-CSF, the number of BrdU positive cells (n=4-7, $F_{(6, 29)}$=48.32, p<0.01) and the ratio of BrdU/DCX double-positive cells (n=4-7, $F_{(6, 29)}$=15.34, p<0.01) in the ICA-CSF group were significantly increased.

3.4 TMT proteomics screening results

3.4.1 DEPs in the CSF of CUMS rats

It was showed that 1935 DEPs were screened between the CON group and the CUMS group. According to the standard of fold change (CUMS/CON or ICA/CUMS)≥1.2 (or ≤0.83) and P-value≤0.05, 100 significantly DEPs were selected (**shown in Table 1**). Among them, 66 proteins were upregulated compared with the CON group and 34 proteins were downregulated (**See Table S1 for details**). The results of the GO annotation of these 100

proteins showed that these proteins were involved in binding, catalytic activity, structural molecule activity, molecular function regulator and transcription regulator activity. The biological process they mainly participated in were cellular process, metabolic process, biological regulation, regulation of biological process and response to stimulus. The result of the KEGG pathway annotation indicated that these 100 DEPs were mostly involved in ribosome, fluid shear stress and atherosclerosis, transcriptional misregulation in cancer, aminoacyl-tRNA biosynthesis and estrogen signaling pathway (**as shown in Figure 6**).

3.4.2 DEPs regulated by both CUMS and ICA

52 DEPs regulated by CUMS and ICA were identified（**Figure 7A and Table 1**）. Among them, 44 DEPs were up-regulated by CUMS and down-regulated by ICA; 8 DEPs were down-regulated by CUMS and up-regulated by ICA. The results of the GO annotation of these 52 DEPs showed that they were involved in the formation of cellular components such as cytoplasm, organelles, and cell membrane. They mainly participate in molecular functions such as nucleic acid binding, protein binding, structural composition of ribosomes, and biological processes such as stress response, biological metabolism and gene expression (**Table S2**). The result of the KEGG pathway annotation indicated that these 100 DEPs were mostly involved in the ribosome pathway, PI3K-Akt signaling pathway and IL-17 signaling pathway (**Figure 7B**).

3.4.3 Quantification of target proteins by PRM

Based on the results of GO annotation and KEGG enrichment analysis, 10 cell proliferation relating DEPs (Rps3, Rps12, Rps4x, Rps14, Rps19, Hsp90b1, Hsp90aa1, Calm1, Cpd and HtrA1) were selected to be analyzed by PRM. The results showed that Rps4x, Rps12, Rps14, Rps19, Hsp90b1 and Hsp90aa1 were up-regulated by CUMS and down-regulated by ICA; HtrA1 was down-regulated by CUMS and up-regulated by ICA (**Table 2**). The PRM results of such 7 proteins were consistent with TMT results, indicating the TMT results were reliable. In addition, Rps3, Calm1 and Cpd were not validated by PRM in this study.

4. Discussion

Depression is highly prevalent in the general population and is associated with grave consequences, including excessive mortality, disability, secondary morbidity and high socioeconomic costs. However, the efficacy of current antidepressant is not optimistic –almost 40% of patients do not recover following an antidepressant trial[4]. Scholars have been devoting themselves to exploring the pathogenesis of depression in an attempt to find more effective and safer antidepressants. Currently, there is an increasing interest in anti-depression effects of natural compounds due to their lower toxicity and diverse biological properties. In this study, it has been observed that ICA showed significant anti-depressant efficacy in depressive-like rats by alleviating typical depressive symptoms such as anhedonia, decreased locomotor activity and despair.

The hippocampus is vulnerable to be damaged from a variety of psychological stressors[22]. Clinically, depressed individuals exhibit cognitive impairment such as memory and learning deficits, implicating hippocampal dysfunction in the pathophysiology of depression. Hippocampal neurogenesis dysfunction is one of the main pathogenesis of depression. Therefore, how to alleviate hippocampal damage is currently a concern of anti-depression research. In this study, ICA showed significant effect in repairing hippocampal damage, learning-memory deficit, hippocampal neurogenesis dysfunction and neuron deletion in DG of depression rats.

ICA could not effectively cross through the blood-brain barriers and accumulate in the brain[12]. Therefore, how ICA exerts anti-depression and anti-hippocampal damage effects has aroused our interest. CSF is the pivot that connects CNS with the periphery and other brain regions, in which substances might directly regulate hippocampal neurogenesis. It was speculated that ICA probably protected hippocampal neurogenesis and promoted neuronal survival by changing CSF components.

To prove this hypothesis, *in vitro*, the chronic stress-induced damage of NSCs was simulated under the high-CORT concentration. It was observed that high-CORT concentration could significantly inhibit the proliferation and differentiation of NSCs. The CSF of CUMS rats could not repair the CORT-induced injuries, while the CSF of ICA rats could effectively resist the damage. The results suggested that ICA might adjust some components in CSF to regulate the proliferation and differentiation of NSCs.

Proteins are the specific executor of life activities and biological functions. Changes in CSF proteomics may be involved in the regulation of ICA on the proliferation and differentiation of NSCs. A total of 52 significantly differential expressed proteins in CSF co-regulated by CUMS and ICA were screened in CSF proteomics in this study. Among these proteins, 44 were up-regulated in CUMS exposure and down-regulated after ICA intervention, while 8 were the down-regulated in CUMS exposure and up-regulated after ICA intervention.

The GO annotation and KEGG pathway enrichment of common DEPs indicated that three possible pathways were involved in the efficacies of ICA in anti-depression, against dysfunctional neurogenesis and neuron deletion, namely ribosome pathway, PI3K-Akt signal pathway and IL-17 signal pathway. To support the TMT analysis results, PRM quantitative analysis was conducted on 10 DEPs that were closely connected with cell proliferation and survival. It had been verified that the regulatory trends of 7 DEPs (Rps4x, Rps12, Rps14, Rps19, Hsp90b1, Hsp90aa1 and Htra1) were consistent with the TMT results.

(1) Proteins related to ribosome pathway

Among the 52 significantly DEPs co-regulated by CUMS and ICA, 11 of them were enriched into the ribosome pathway, which was the most enriched KEGG pathway. All these 11 proteins in CSF were up-regulated by CUMS.

A large number of studies have confirmed that abnormal ribosomal proteins expression or transcription exists in patients with depression and animal models. Most of such studies have observed that the expression of ribosomal proteins is up-regulated or increased transcription in blood, liver, hippocampus and other tissues of depressed individuals[23-25]. It has been also observed that the expression of ribosomal proteins in the hippocampus of rats was significantly down-regulated under 3-week exposure to CUMS[26]. According to our previous study [4], although rats showed depression-like behaviors after 3-week exposure to CUMS, rats were still in the stress compensation stage, which did not cause hippocampal damage. Different brain regions may not respond to mental stress simultaneously and may react differently towards various stressors. Nevertheless, abnormal expression or transcription of ribosomal proteins is found in both central and peripheral regions of depressed individuals.

It is worth noting that in PRM analysis, the expressed differences of ribosomal proteins showed higher significance than in high-throughput TMT results. It was suggested that these ribosomal proteins might play an important role in the development and remission of depression.

Ribosomes are consisting of ribosomal RNAs and ribosomal proteins and are the main sites for intracellular RNA translation controlling protein synthesis. During the stress process, to cope against stress-induced damages, the assembly of ribosomes and synthesis of proteins speed up as the demand for proteins increases[27-29]. In this study, more up-expressed DEPs rather than down-expressed ones were observed in the CSF of CUMS rats.

However, ribosome assembly requires extremely high rates, coordinated synthesis and assembly of macromolecules across cellular compartments. Ribosomal synthesis dysfunction may easily appear under stimulates during the assembly process, resulting in rapid accumulation of ribosomal proteins[30-32]. In addition, numerous studies have shown that multiple cellular stresses could directly act on the nucleus and trigger the overexpression of ribosomal proteins. Therefore, the overexpression of ribosomal proteins may indicate ribosomal assembly dysfunction under stress[33, 34].

Ribosomes control the translation of all proteins in cells, the normal synthesis of ribosome is essential for cell survival, growth and proliferation. In the process of ribosome synthesis, either over-expression or under-expression of ribosomal protein could disrupt ribosome synthesis, lead to ribosomal assembly dysfunctions and cause cell cycle arrest, senescence or apoptosis[35]. In addition, the accumulation of ribosomal proteins caused by the ribosome synthesis dysfunction could lead to protein folding homeostasis collapse, inhibiting cell growth[31, 32]. It may also cause cell cycle arrest or apoptosis through extraribosomal functions of ribosomal proteins[36]. For example, Rps14 activates p53 pathway to inhibit cell proliferation and induce apoptosis[37]. In the CNS, the normal synthesis of ribosome also plays an important role in the development of neurons. Some forms of synaptic plasticity require rapid, local activation of protein synthesis in ribosome[38]. Dysfunction in ribosomal gene expression may be associated with a decrease of proliferation in DG[39].

In this study, multiple increased ribosomal proteins (including Rps4x, Rps12, Rps14, Rps19) in CSF of depression rats suggested ribosomal synthesis dysfunction in depression rats, which may be related to neurogenesis dysfunction and neuronal loss in DG. ICA could significantly down-regulate the expression of such ribosomal proteins in CSF of depression rats, promote the normal synthesis of ribosome, provide more proteins needed for the repair of neurons, proliferation and differentiation of NSCs.

In summary, ribosomal synthesis dysfunction may affect cell proliferation and survival by abnormal expression of ribosomal proteins. ICA may resist neurogenesis dysfunction and neuronal loss in rats with depression by repairing ribosomal synthesis dysfunction.

(2) Proteins related to PI3K-Akt pathway and IL-17 pathway

PI3K-Akt pathway is one of the classical pathways regulating cell cycle, which is of great significance in promoting the survival of neurons and neurogenesis [40]. It is also one of the effective pathways of many antidepressants[41, 42]. Hsp90b1 and Hsp90aa1 are important proteins and targets in the PI3K-Akt pathway. Abnormal expression of Hsp90b1 and Hsp90aa1 could both inhibit PI3K-Akt pathway activity [43, 44]. Chronic stress could cause overexpression of HSP90 family proteins in the brain of depression animals[45], and overexpressed Hsp90b1 and Hsp90aa1 would combine with HIF1α to promote NDRG2 expression and play a key negative regulatory role in PI3K-Akt signaling[43].

Hsp90b1 and Hsp90aa1 are also important members of the IL-17 pathway. HSP90 functions as a chaperone that facilitates the folding and assembly of its client proteins. Loss of HSP90 chaperone function results in the

degradation of its client proteins—Act1. As Act1 is required for IL-17 signaling and is a client protein of heat shock protein 90 (Hsp90) family proteins, so that Hsp90 activity is required for IL-17 signaling[46]. Epithelial cells, endothelial cells and glial cells are all target cells of IL-17. IL-17 is activated after binding to the receptors of target cells and ultimately promotes the release of large amounts of inflammatory cytokines from target cells, which is one of many causes of neuronal death in individuals with depression[47]. In addition, some pathological phenomena induced by IL-17 can be reversed by inhibiting the activity of Hsp90 family proteins[48].

In this study, PI3K-Akt pathway and IL-17 pathway were enriched, Hsp90b1 and Hsp90aa1 were overexpressed in CSF, neurogenesis dysfunction and hippocampal neuronal loss were observed in depression rats. It was suggested that the overexpressed Hsp90b1 and Hsp90aa1 might inhibit PI3K-Akt pathway and activate IL-17 pathway in hippocampus, causing neurogenesis dysfunction and neuronal loss in depression rats. The efficacy of ICA in repairing neurogenesis dysfunction and neuronal loss may be related to the reduction of Hsp90b1 and Hsp90aa1 in CSF.

In addition, though not enriched in KEGG pathway, some DEPs co-regulated by CUMS and ICA may be involved in repairment of dysfunctional neurogenesis and neural reduction. For example, HtrA serine peptidase 1 (HtrA1) is abundantly expressed in astrocytes. Down-expressed HtrA1 is related to a variety of neurological diseases. HtrA1 could mediate transforming growth factor-β hydrolysis and bone morphogenetic protein inhibition to prevent neural stem cell proliferation and differentiation inhibition[49]. In this study, the treatment of ICA reversed CUMS-induced Htra1 reduction in CSF, neurogenesis dysfunction and neuronal loss in DG, suggesting that the anti-hippocampal damage effect of ICA may be related to the regulation of Htra1 content in CSF.

In conclusion, 6-week ICA intervention could significantly alleviate the hippocampal neurogenesis dysfunction, neuronal loss in DG and memory and learning deficits in depression rats. Such efficacies of ICA may be related to its regulation of Rps14, Hsp90b1, Htra1 and other proteins in CSF. The pathways involved mainly include ribosome pathway, PI3K-Akt pathway and IL-17 pathway. It was suggested that ICA might protect hippocampus by changing CSF proteomics (**as shown in Figure 8**).

Conclusions

This study showed prospect of ICA as a potential antidepressant, but there remain some problems. The pathways and targets of ICA in anti-hippocampal damage screened in this study need to be further verified. As we known, brain metabolites could directly transfer into the CSF. It cannot be ruled out that a small amount of ICA crossing the blood-brain barrier might affect brain regions' metabolism and lead to the changing of CSF proteomics.

Abbreviations

4',6-diamidino-2-phenylindole, DAPI; 5-Bromo-2-deoxyUridine, BrdU; cell counting kit-8, CCK-8; central nervous system, CNS; cerebrospinal fluid, CSF; chronic unpredictable mild stress, CUMS; corticosterone, CORT; differentially expressed proteins, DEPs; doublecortin, DCX; forced swimming test, FST; Gene Ontology, GO;

Icariin, ICA; Kyoto Encyclopedia of Genes and Genomes, KEGG; neural stem cells, NSCs; open field test, OFT; parallel reaction monitoring, PRM; sucrose preference test, SPT; Tandem mass tag, TMT.

Declarations

Ethics approval and consent to participate:

All experimental procedures and protocols were approved by the Experimental Animal Ethics Committee of Guangzhou University of Chinese Medicine of China. The experimental procedure followed the United States National Institutes of Health Guide for the Care and Use of Laboratory Animals (NIH Publication No. 85 – 23, revised 1996).

Consent for publication:

The manuscript does not contain any individual person's data in any form.

Availability of data and materials :

The Differentially expressed proteinsis presented in Tables 1, and the dataset used and/ or analyzed in this study is available from the corresponding author on reasonable request.

Competing interests:

The authors declare no confict of interest.

Funding:

This study was supported by the National Natural Science Foundation of China, No. 81774102 (to LL W).

Authors' contributions

Ning-Xi Zeng analyzed data, drafted fgures, wrote and revised the manuscript; Hui-Zhen Li performed some data analysis, drafted part of the manuscript, some fgures and figure legends;Han-Zhang Wang isolated brain and dissected animal tissues and wrote parts of the manuscript; Kai-Ge Liu performed CUMS procedures and wrote parts of the manuscript; Xia-Yu Gong performed CUMS procedures and some data analysis; Wu-Long Luo performed CUMS procedures; Li-Li Wu and Can Yan conceived the experiments and contributed to writing of the manuscript. All authors read and approved the fnal manuscript.

Acknowledgment

The study was supported by Research Center for Basic Integrative Medicine, Guangzhou University of Chinese Medicine.

References

1. Bachmann S. Epidemiology of Suicide and the Psychiatric Perspective. Int J Env Res Pub He. 2018;15(7).

2. O'Leary OF, Cryan JF. A ventral view on antidepressant action: roles for adult hippocampal neurogenesis along the dorsoventral axis. Trends Pharmacol Sci. 2014;35(12):675–87.
3. Park SC. Neurogenesis and antidepressant action. Cell Tissue Res. 2019;377(1):95–106.
4. Huang YL, Zeng NX, Chen J, Niu J, Luo WL, Liu P, et al. Dynamic changes of behaviors, dentate gyrus neurogenesis and hippocampal miR-124 expression in rats with depression induced by chronic unpredictable mild stress. Neural Regeneration Research. 2020;15(6):1150–59.
5. Maller JJ, Daskalakis ZJ, Fitzgerald PB. Hippocampal volumetrics in depression: The importance of the posterior tail. Hippocampus. 2007;17(11):1023–27.
6. Danzer SC. Depression, stress, epilepsy and adult neurogenesis. Exp Neurol. 2012;233(1):22–32.
7. Duman RS, Aghajanian GK. Synaptic Dysfunction in Depression: Potential Therapeutic Targets. Science. 2012;338(6103):68–72.
8. Wu LL, Ran CL, Liu SK, Liao LZ, Chen YL, Guo HL, et al. Jiaweisinisan facilitates neurogenesis in the hipp campus after stress damage. Neural Regeneration Research. 2013;8(12):1091–102.
9. Liu B, Xu C, Wu X, Liu F, Du Y, Sun J, et al. Icariin Exerts an Antidepressant Effect in an Unpredictable Chronic Mild Stress Model of Depression in Rats and Is Associated with the Regulation of Hippocampal Neuroinflammation. Neuroscience. 2015;294:193–205.
10. Wei K, Xu YZ, Zhao ZX, Wu X, Du YJ, Sun J, et al. Icariin alters the expression of glucocorticoid receptor, FKBP5 and SGK1 in rat brains following exposure to chronic mild stress. Int J Mol Med. 2016;38(1):337–44.
11. Liu LM, Zhao ZX, Lu LW, Liu JQ, Sun J, Dong JC. Icariin and icaritin ameliorated hippocampus neuroinflammation via mediating HMGB1 expression in social defeat model in mice. Int Immunopharmacol. 2019;75.
12. Xu SJ, Yu JJ, Zhan JJ, Yang L, Guo LG, Xu YJ. Pharmacokinetics, Tissue Distribution, and Metabolism Study of Icariin in Rat. Biomed Research International. 2017;2017.
13. Lepko T, Pusch M, Muller T, Schulte D, Ehses J, Kiebler M, et al. Choroid plexus-derived miR-204 regulates the number of quiescent neural stem cells in the adult brain. Embo J. 2019;38:17.
14. Planques A, Moreira VO, Dubreuil C, Prochiantz A, Di Nardo AA. OTX2 Signals from the Choroid Plexus to Regulate Adult Neurogenesis. Eneuro. 2019;6(2).
15. Skipor J, Thiery JC. The choroid plexus - cerebrospinal fluid system: Undervaluated pathway of neuroendocrine signaling into the brain. Acta Neurobiol Exp. 2008;68(3):414–28.
16. Ogawa S, Tsuchimine S, Kunugi H. Cerebrospinal fluid monoamine metabolite concentrations in depressive disorder: A meta-analysis of historic evidence. J Psychiatr Res. 2018;105:137–46.
17. Qin YH, Jiang XF, Li W, Li J, Tian T, Zang GC, et al. Chronic mild stress leads to aberrant glucose energy metabolism in depressed Macaca fascicularis models. Psychoneuroendocrino. 2019;107:59–69.
18. Ditzen C, Tang N, Jastorff AM, Teplytska L, Yassouridis A, Maccarrone G, et al. Cerebrospinal Fluid Biomarkers for Major Depression Confirm Relevance of Associated Pathophysiology. Neuropsychopharmacol. 2012;37(4):1013–25.
19. Al Shweiki MHDR, Oeckl P, Steinacker P, Hengerer B, Schonfeldt-Lecuona C, Otto M. Major depressive disorder: insight into candidate cerebrospinal fluid protein biomarkers from proteomics studies. Expert Rev Proteomic. 2017;14(6):499–514.

20. Wu LL, Liu Y, Yan C, Pan Y, Su JF, Wu WK. Antidepressant-Like Effects of Fractions Prepared from Danzhi-Xiaoyao-San Decoction in Rats with Chronic Unpredictable Mild Stress: Effects on Hypothalamic-Pituitary-Adrenal Axis, Arginine Vasopressin, and Neurotransmitters. Evid-Based Compl Alt. 2016.
21. Yujie Y, Yujiao L, Shanshan L, Xinmin L, Qiong W. 2018.Comparison of experimental maze tests used to assess the learning and memory abilities in rats and mice. Chinese Journal of Comparative Medicine. 2018;28(12):129 – 34.
22. Oitzl MS, Fluttert M, de Kloet ER. Acute blockade of hippocampal glucocorticoid receptors facilitates spatial learning in rats. Brain Res. 1998;797(1):159–62.
23. Li C, Guo ZG, Zhao RH, Sun W, Xie M. Proteomic Analysis of Liver Proteins in a Rat Model of Chronic Restraint Stress-Induced Depression. Biomed Research International. 2017;2017.
24. Hori H, Nakamura S, Yoshida F, Teraishi T, Sasayama D, Ota M, et al. Integrated profiling of phenotype and blood transcriptome for stress vulnerability and depression. J Psychiatr Res. 2018;104:202–10.
25. Guo JJ, Zhang F, Gao JF, Guan XY, Liu BY, Wang XG, et al. Proteomics-based screening of the target proteins associated with antidepressant-like effect and mechanism of Saikosaponin A. J Cell Mol Med. 2020;24(1):174–88.
26. Zhang JL, Zhang ZN, Zhang JP, Zhong Z, Yao ZY, Qu SS, et al. iTRAQ-Based Protein Profiling in CUMS Rats Provides Insights into Hippocampal Ribosome Lesion and Ras Protein Changes Underlying Synaptic Plasticity in Depression. Neural Plast. 2019;2019.
27. Spriggs KA, Bushell M, Willis AE. Translational Regulation of Gene Expression during Conditions of Cell Stress. Mol Cell. 2010;40(2):228–37.
28. Vadivel Gnanasundram S, Fahraeus R. Translation Stress Regulates Ribosome Synthesis and Cell Proliferation. Int J Mol Sci. 2018;19(12).
29. Wu CC, Zinshteyn B, Wehner KA, Green R. High-Resolution Ribosome Profiling Defines Discrete Ribosome Elongation States and Translational Regulation during Cellular Stress. Mol Cell. 2019;73(5):959–70. e5.
30. Warner JR. The economics of ribosome biosynthesis in yeast. Trends Biochem Sci. 1999;24(11):437–40.
31. Lempiainen H, Shore D. Growth control and ribosome biogenesis. Curr Opin Cell Biol. 2009;21(6):855–63.
32. Tye BW, Commins N, Ryazanova LV, Wuhr M, Springer M, Pincue D, et al. Proteotoxicity from aberrant ribosome biogenesis compromises cell fitness. Elife. 2019;8.
33. Zhang YP, Lu H. Signaling to p53: Ribosomal Proteins Find Their Way. Cancer Cell. 2009;16(5):369–77.
34. Zhou X, Liao JM, Liao WJ, Lu H. Scission of the p53-MDM2 Loop by Ribosomal Proteins. Genes Cancer. 2012;3(3–4):298–310.
35. Turi Z, Lacey M, Mistrik M, Moudry P. Impaired ribosome biogenesis: mechanisms and relevance to cancer and aging. Aging-Us. 2019;11(8):2512–40.
36. Zhou X, Liao WJ, Liao JM, Liao P, Lu H. Ribosomal proteins: functions beyond the ribosome. J Mol Cell Biol. 2015;7(2):92–104.
37. Zhou X, Hao Q, Liao J, Zhang Q, Lu H. Ribosomal protein S14 unties the MDM2-p53 loop upon ribosomal stress. Oncogene. 2013;32(3):388–96.
38. Graber TE, Hebert-Seropian S, Khoutorsky A, David A, Yewdell JW, Lacaille JC, et al. Reactivation of stalled polyribosomes in synaptic plasticity. P Natl Acad Sci USA. 2013;110(40):16205–10.

39. Smagin DA, Kovalenko IL, Galyamina AG, Bragin AO, Orlov YL, Kudryavtseva NN. Dysfunction in Ribosomal Gene Expression in the Hypothalamus and Hippocampus following Chronic Social Defeat Stress in Male Mice as Revealed by RNA-SEq. Neural Plast. 2016;2016.
40. Manning BD, Toker A. AKT/PKB Signaling: Navigating the Network. Cell. 2017;169(3):381–405.
41. Huang X, Mao YS, Li C, Wang H, Ji JL. Venlafaxine inhibits apoptosis of hippocampal neurons by up-regulating brain-derived neurotrophic factor in a rat depression model. Pharmazie. 2014;69(12):909–16.
42. Pazini FL, Cunha MP, Rosa JM, Colla ARS, Lieberknecht V, Oliveira A, et al. Creatine, Similar to Ketamine, Counteracts Depressive-Like Behavior Induced by Corticosterone via PI3K/Akt/mTOR Pathway. Mol Neurobiol. 2016;53(10):6818–34.
43. Ichikawa T, Nakahata S, Tamura T, Manachai N, Morishita K. The loss of NDRG2 expression improves depressive behavior through increased phosphorylation of GSK3 beta. Cell Signal. 2015;27(10):2087–98.
44. Giulino-Roth L, van Besien HJ, Dalton T, Totonchy JE, Rodina A, Taldone T, et al. Inhibition of Hsp90 Suppresses PI3K/AKT/mTOR Signaling and Has Antitumor Activity in Burkitt Lymphoma. Mol Cancer Ther. 2017;16(9):1779–90.
45. Zhang Y, Du LF, Bai Y, Han B, He CC, Gong L, et al. CircDYM ameliorates depressive-like behavior by targeting miR-9 to regulate microglial activation via HSP90 ubiquitination. Mol Psychiatr. 2020;25(6):1175–90.
46. Kim BK, Park M, Kim JY, Lee KH, Woo SY. Heat shock protein 90 is involved in IL-17-mediated skin inflammation following thermal stimulation. Int J Mol Med. 2016;38(2):650–58.
47. Nadeem A, Ahmad SF, Al-Harbi NO, Fardan AS, El-Sherbeeny AM, Ibrahim KE, et al. IL-17A causes depression-like symptoms via NF kappa B and p38MAPK signaling pathways in mice: Implications for psoriasis associated depression. Cytokine. 2017;97:14–24.
48. Pezzulo AA, Tudas RA, Stewart CG, Buonfiglio LGV, Lindsay BD, Taft PJ, et al. HSP90 inhibitor geldanamycin reverts IL-13-and IL-17-induced airway goblet cell metaplasia. J Clin Invest. 2019;129(2):744–58.
49. Chen J, Van Gulden S, McGuire TL, Fleming AC, Oka C, Kessler JA, et al. BMP-Responsive Protease HtrA1 Is Differentially Expressed in Astrocytes and Regulates Astrocytic Development and Injury Response. J Neurosci. 2018;38(15):3840–57.

Tables

Table 1 Differentially expressed proteins of CSF regulated by CUMS and ICA

Accession	Protein Name	Gene Name	CON/CUMS	ICA/CUMS
ENSRNOP00000002394	chordin	Chrd	1.330657	1.251991
ENSRNOP00000004386	myocilin	Myoc	1.237837	1.321273
ENSRNOP00000012286	UDP-GlcNAc:betaGalbeta-1,3-N-acetylglucosaminyltransferase 2	B3gnt2	1.346536	1.214411
ENSRNOP00000016389	transforming growth factor, beta induced	Tgfbi	1.246915	1.206508
ENSRNOP00000027860	HtrA serine peptidase 1	Htra1	1.246935	1.239292
ENSRNOP00000059194	angiopoietin-like 1	Angptl1	1.294498	1.220162
ENSRNOP00000070498	carboxypeptidase D	Cpd	1.320809	1.340595
ENSRNOP00000071077	collagen type II alpha 1 chain	Col2a1	1.836686	1.680284
ENSRNOP00000001397	transmembrane p24 trafficking protein 2	Tmed2	0.473675	0.404166
ENSRNOP00000001518	ribosomal protein lateral stalk subunit P0	Rplp0	0.696513	0.706795
ENSRNOP00000004278	ribosomal protein S4, X-linked	Rps4x	0.353676	0.372436
ENSRNOP00000004867	small ubiquitin-like modifier 2	Sumo2	0.746357	0.557202
ENSRNOP00000008509	eukaryotic translation initiation factor 1A, X-linked	Eif1ax	0.658648	0.648145
ENSRNOP00000009249	proteasome 26S subunit, non-ATPase 6	Psmd6	0.550629	0.486541
ENSRNOP00000009556	heat shock protein HSP 90-alpha	HSP90AA1	0.730779	0.665003
ENSRNOP00000009649	proteasome 26S subunit, ATPase 6	Psmc6	0.718329	0.621687
ENSRNOP00000010674	tyrosyl-tRNA synthetase	Yars	0.556245	0.649364
ENSRNOP00000013375	eukaryotic translation initiation factor 2 subunit alpha	Eif2s1	0.465363	0.499192
ENSRNOP00000015598	RAB11a, member RAS oncogene family	Rab11a	0.730942	0.70133
ENSRNOP00000017234	heparin binding growth factor	Hdgf	0.771831	0.595331
ENSRNOP00000019162	ribosomal protein L35	Rpl35	0.61251	0.58689
ENSRNOP00000019247	ribosomal protein L27a	Rpl27a	0.673251	0.666698
ENSRNOP00000021048	myosin light chain 12A	Myl12a	0.495839	0.518126
ENSRNOP00000022184	ribosomal protein S12	Rps12	0.255554	0.234153

ENSRNOP00000022603	calmodulin 1	Calm1	0.636832	0.5501
ENSRNOP00000023935	ribosomal protein S3	Rps3	0.519405	0.502597
ENSRNOP00000024430	vimentin	Vim	0.727629	0.691827
ENSRNOP00000025217	ribosomal protein L17	Rpl17	0.482482	0.50053
ENSRNOP00000026528	ribosomal protein S5	Rps5	0.414189	0.469701
ENSRNOP00000026696	heat shock protein family A member 9	Hspa9	0.679796	0.621869
ENSRNOP00000027246	ribosomal protein S19	Rps19	0.452858	0.524735
ENSRNOP00000033144	ribosomal protein s25	Rps25	0.364721	0.310551
ENSRNOP00000033950	ubiquitin-like modifier activating enzyme 1	Uba1	0.787971	0.715948
ENSRNOP00000034657	ubiquitin-like protein fubi and ribosomal protein S30-like	LOC100360647	0.392441	0.374892
ENSRNOP00000034846	heat shock protein 90 beta family member 1	Hsp90b1	0.735841	0.802234
ENSRNOP00000038448	seryl-tRNA synthetase	SerRS	0.517425	0.483297
ENSRNOP00000044296	actin, beta	Actb	0.783141	0.768301
ENSRNOP00000056260	ribosomal protein S14	Rps14	0.523183	0.572311
ENSRNOP00000060949	ribosomal protein L34	Rpl34	0.150869	0.172269
ENSRNOP00000064424		AABR07065778.2	0.593477	0.614344
ENSRNOP00000066331		AABR07065750.2	0.581222	0.541466
ENSRNOP00000067217	histone cluster 1 H2a family member l like 1	Hist1h2ail1	0.491005	0.388903
ENSRNOP00000070331	protein kinase N3	Pkn3	0.455886	0.407136
ENSRNOP00000070868	tubulin, alpha 1B	Tuba1b	0.689164	0.596259
ENSRNOP00000071233	spectrin, beta, non-erythrocytic 1	Sptbn1	0.670589	0.628294
ENSRNOP00000072016	TATA-box binding protein associated factor 15	Taf15	0.693424	0.622737
ENSRNOP00000073493	RAB1A, member RAS oncogene family	Rab1a	0.579087	0.532868
ENSRNOP00000074005	dyskerin pseudouridine synthase 1	Dkc1	0.13148	0.139895
ENSRNOP00000074688	ubiquitin C	Ubc	0.733036	0.750576
ENSRNOP00000075909	NFKB activating protein	Nkap	0.291945	0.260421

Table 2. PRM quantitative analysis of target proteins.

Protein Name	Gene Name	PRM results		TMT results	
		CUMS / CON	ICA/CUMS	CUMS / CON	ICA/CUMS
HtrA serine peptidase 1	Htra1	0.3347	1.7893	0.8020	1.2393
ribosomal protein S4, X-linked	Rps4x	3.4306	0.8016	2.8274	0.3724
heat shock protein HSP 90-alpha	LOC103692716	3.6841	0.3606	1.3684	0.6650
ribosomal protein S12	Rps12	6.4356	0.4176	3.9131	0.2342
ribosomal protein S19	Rps19	11.4161	0.1136	2.2082	0.5247
heat shock protein 90 beta family member 1	Hsp90b1	3.4992	0.4571	1.3590	0.8022
ribosomal protein S14	Rps14	15.7618	0.0882	1.9114	0.5723

Figures

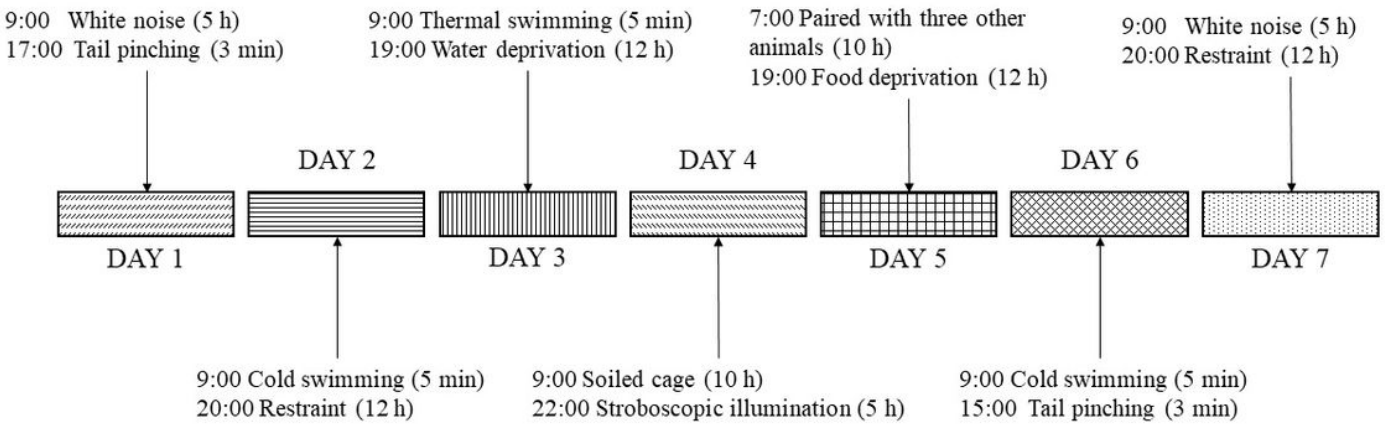

Figure 1

CUMS procedure. One or two arbitrary mild stressors were randomly applied for 6weeks and the same stressors were not scheduled in three consecutive days.

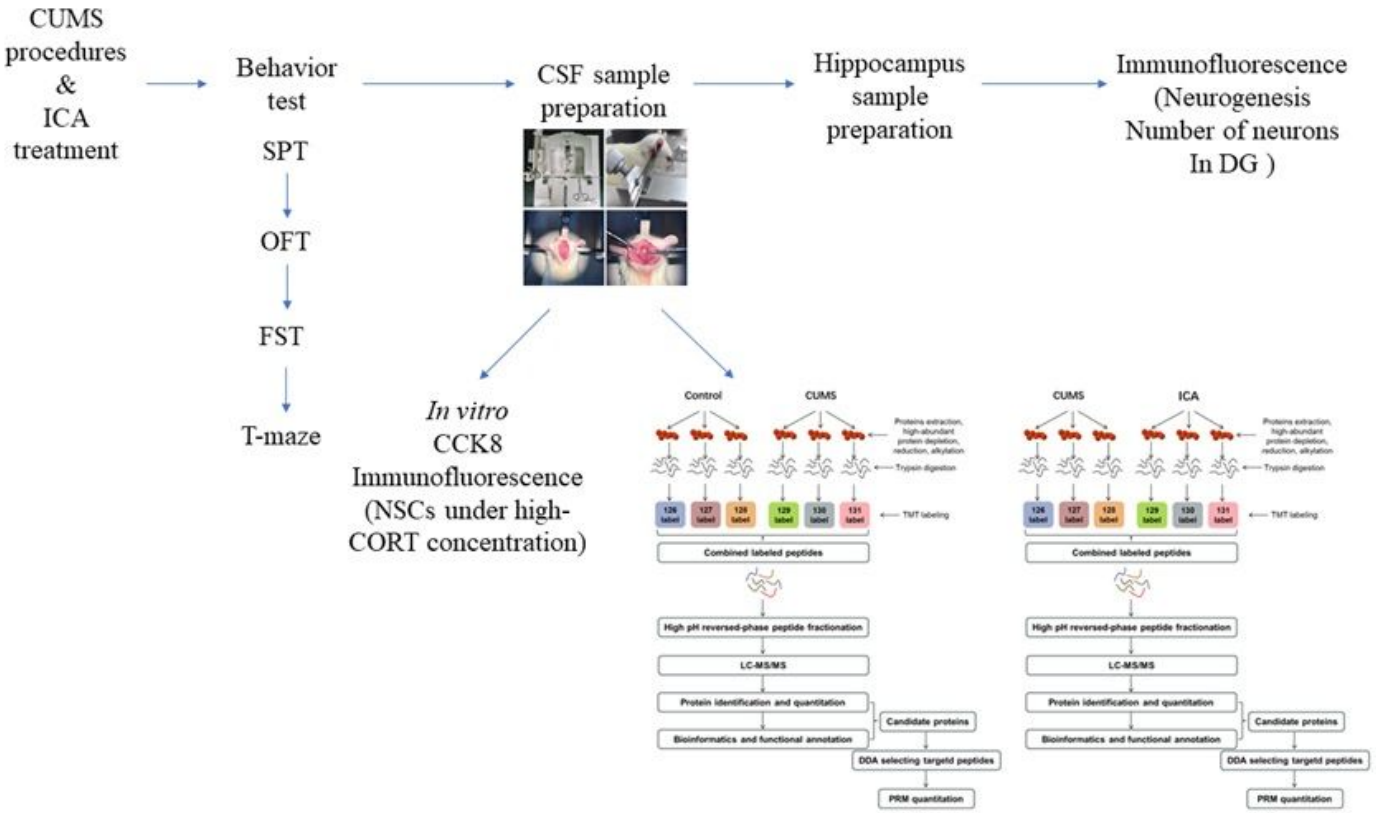

Figure 2

Experiments procedure.

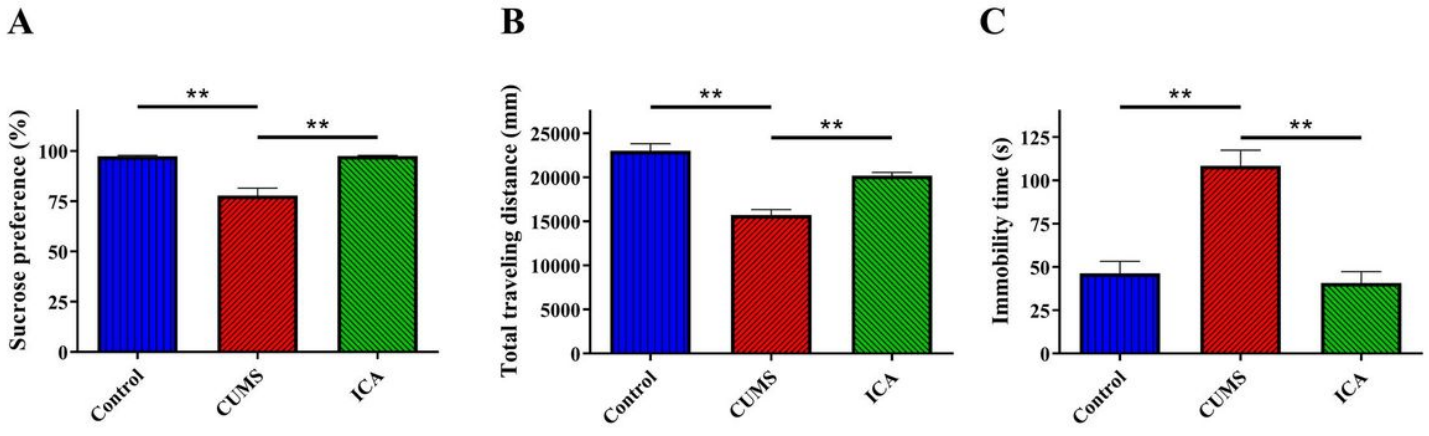

Figure 3

The effect of ICA on behaviors. A)Sucrose preference（SPT）. B) Total traveling distance（OFT）. C) Immobility time (FST). Data were expressed as the mean ± SEM (n = 15 per group). *p＜0.05, **p＜0.01.

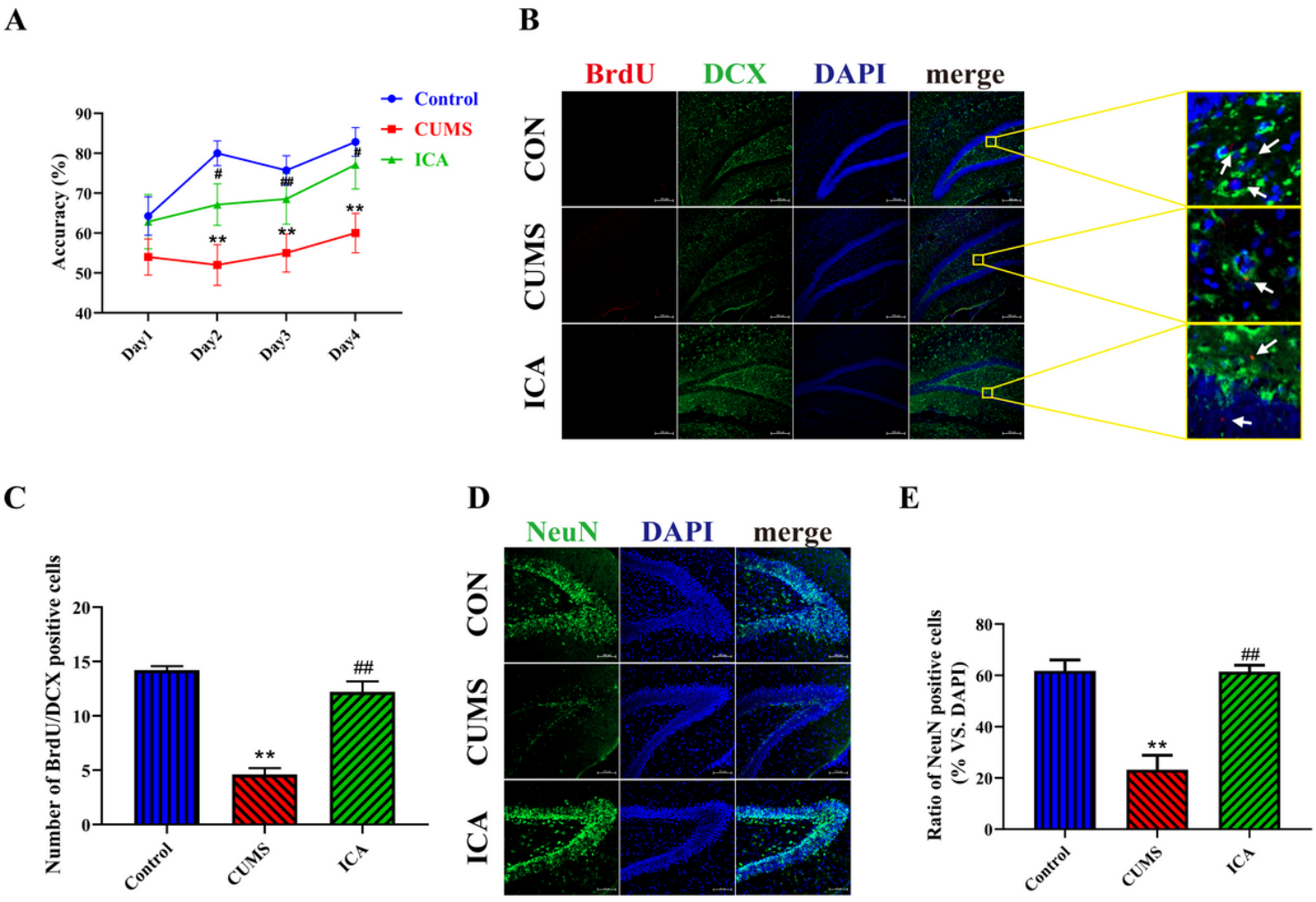

Figure 4

The effect of ICA on hippocampal damage. A) T-maze accuracy (n=8 per group). B) BrdU/DCX positive cells in DG, red: BrdU, green: DCX, blue: DAPI. C) Numbers of BrdU/DCX positive cells in DG (n=5 per group). D) NeuN positive cells in DG, green: NeuN, blue: DAPI. E) Relatively number of neurons in DG (n=5 per group). Data were expressed as the mean ± SEM. *p□0.05, **p□0.01, vs. control. #p□0.05, ##p□0.01, vs. CUMS.

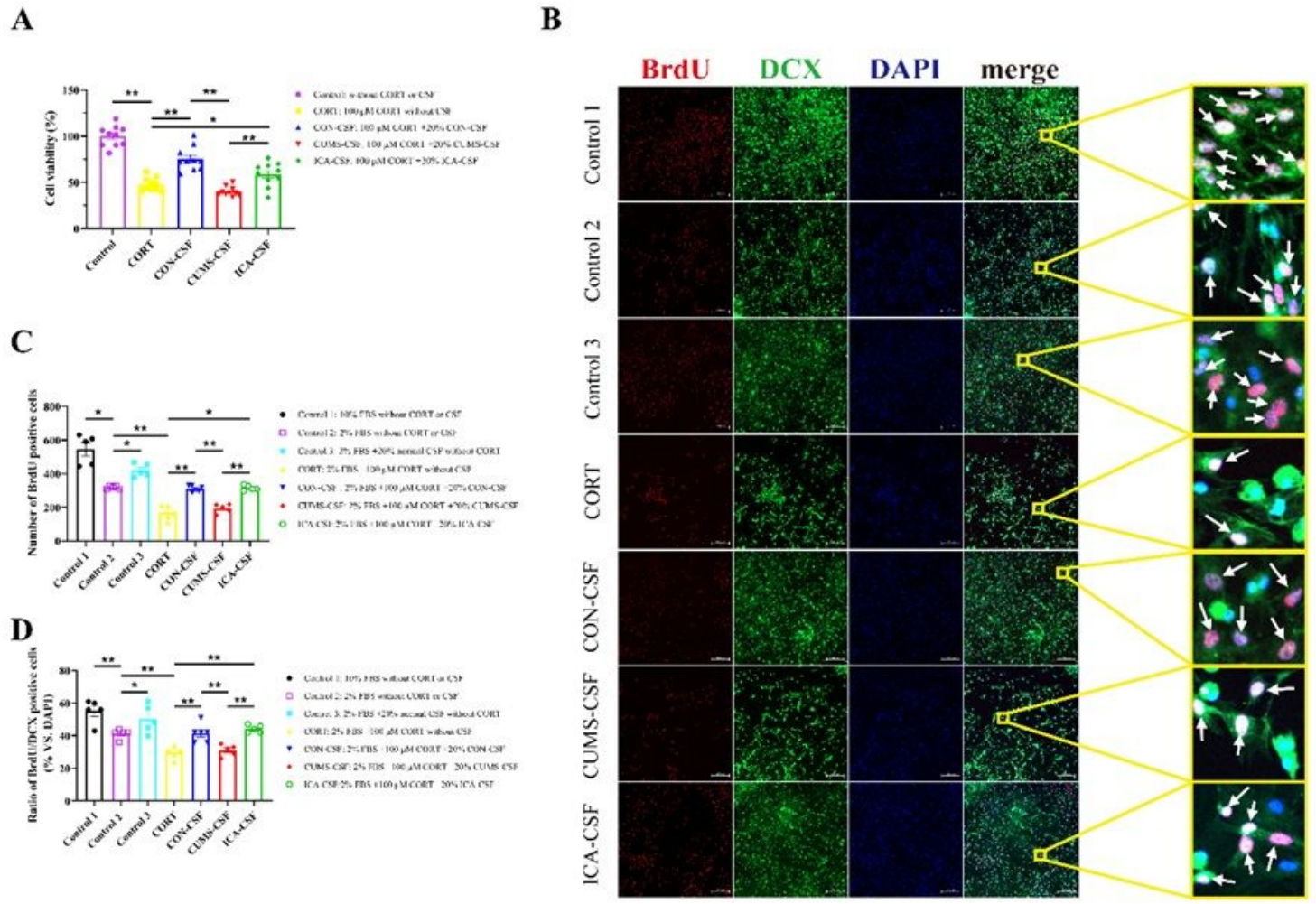

Figure 5

The effect of CSF on primary hippocampal NSCs' proliferation and differentiation into neurons under high-CORT concentration. A) Cell viability (n=10 per group). B) BrdU/DCX positive cells, red: BrdU, green: DCX, blue: DAPI. C) Number of BrdU positive cells (n=5 per group). D) Number of BrdU/DCX double positive cells (n=5 per group). Data were expressed as the mean ± SEM. *p□0.05, **p□0.01.

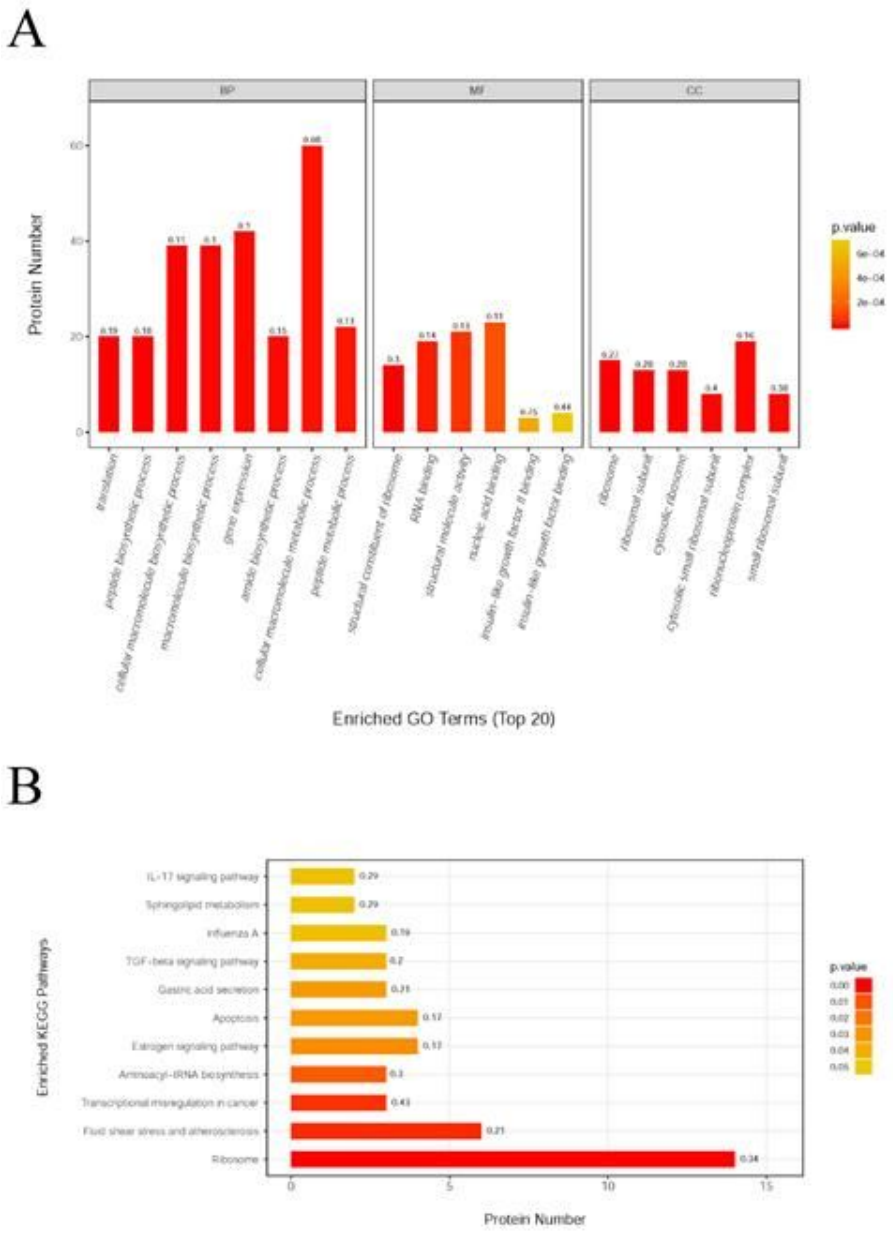

Figure 6

The result of the GO annotation and KEGG pathway enrichment of differentially expressed proteins between the CON and CUMS group. A) GO annotation (TOP 20). B) KEGG pathway enrichment.

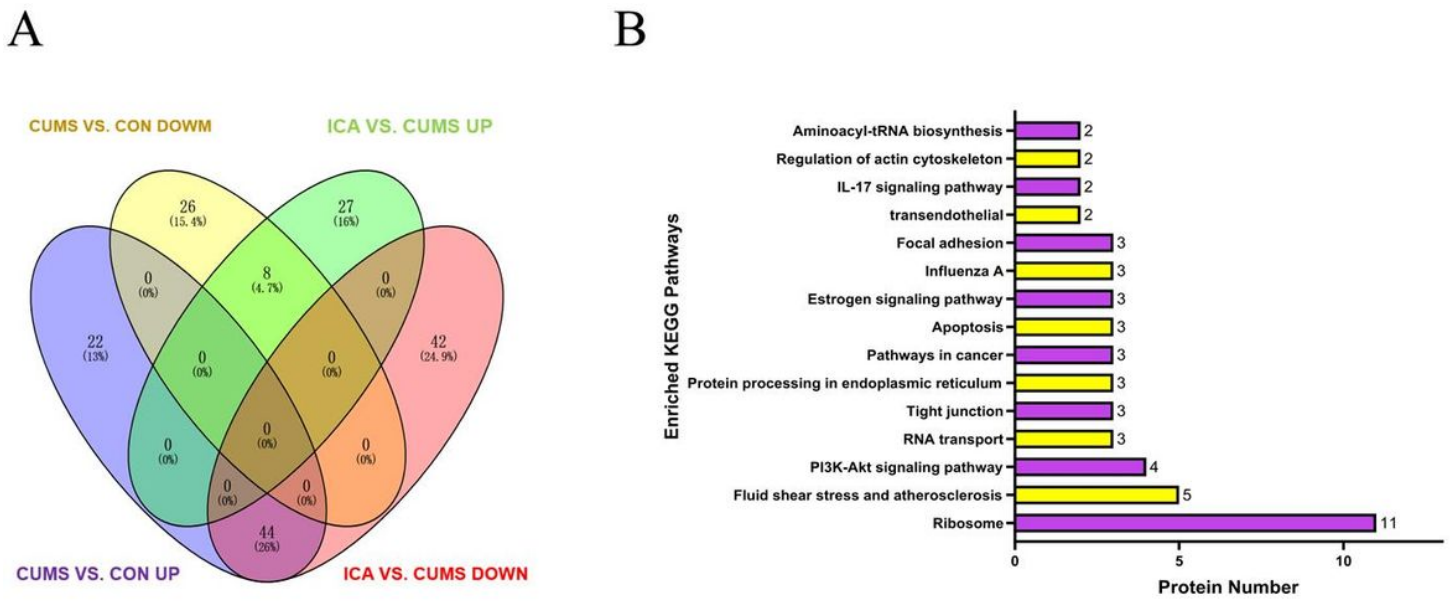

Figure 7

Differentially expressed proteins regulated by both CUMS and ICA, A) VEEN map. B) KEGG pathway enrichment.

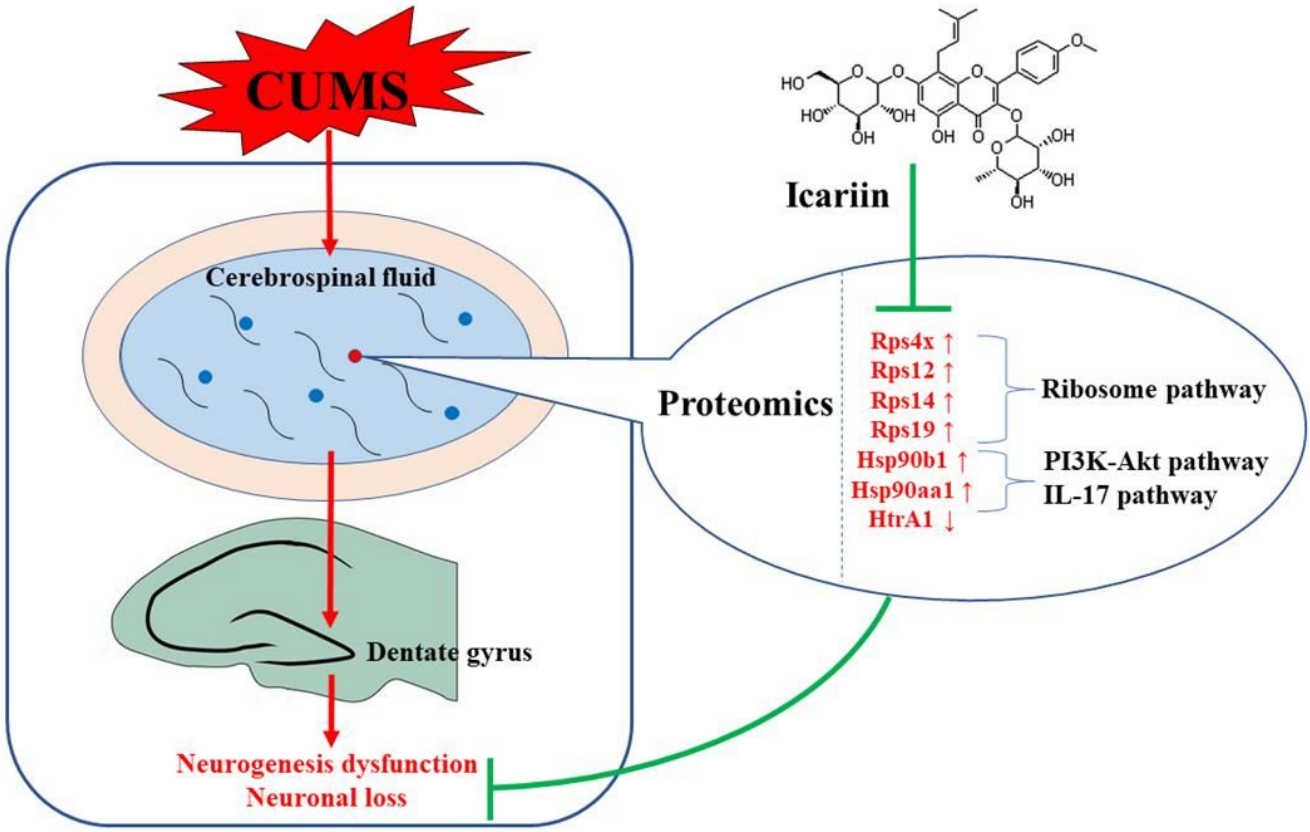

Figure 8

The possible mechanism of ICA against hippocampal neurogenesis dysfunction via CSF in depression.

Supplementary Files

This is a list of supplementary files associated with this preprint. Click to download.

- TableS1100significantlyDEPswereselected..xlsx
- TableS2GOofthese52DEPs..xlsx